Diffractive axicons fabricated by laser direct writer on curved surface

2007 J. Opt. A: Pure Appl. Opt. 9 160

(http://iopscience.iop.org/1464-4258/9/2/007)

INSTITUTE OF PHYSICS PUBLISHING JOURNAL OF OPTICS A: PURE AND APPLIED OPTICS
J. Opt. A: Pure Appl. Opt. **9** (2007) 160–164 doi:10.1088/1464-4258/9/2/007

Diffractive axicons fabricated by laser direct writer on curved surface

Zhenwu Lu[1], Hua Liu[1], Ruiting Wang[2], Fengyou Li[1] and Yichun Liu[3]

[1] State Key Laboratory of Applied Optics, Changchun Institute of Optics, Fine Mechanics and Physics, Changchun 130022, People's Republic of China
[2] College of Mathematics, Jilin University, Changchun 130012, People's Republic of China
[3] School of Physics, Northeast Normal University, Changchun 130022, People's Republic of China

E-mail: luzw@ciomp.cn

Received 8 June 2006, accepted for publication 12 December 2006
Published 4 January 2007
Online at stacks.iop.org/JOptA/9/160

Abstract
We report a computer-generated element: diffractive axicon, which is fabricated by laser beam lithography on a concave lens surface, for obtaining more uniform axial line focus over a long interval, compared with traditional methods. The on-axis intensity distribution of this kind of diffractive axicon fabricated by our laser direct writer was tested and the results agree well with the theoretical analysis.

Keywords: computer-generated element, lithography, diffractive axicon

1. Introduction

Axically symmetric convergence of light rays to a continuous range of points extended along the axis can be arbitrarily called axicon focusing, by association with Mcleod's name for optical elements that perform this function: axicons [1, 2]. It is useful in many applications of this kind of optical element such as in spatial alignment [3], optical pumping of plasma [4], optical readout and processing [5] and laser machining [6]. To produce near-constant axial intensity in the beam centre within a long region, several kinds of methods have been proposed. One is placing a ring aperture with appropriate radius in the focal plane of a positive lens [7]. However, this approach is difficult to utilize due to its low light efficiency, since only a small fraction of incident light is transmitted. The other direct one is using axicons in the form of a conical lens [8, 9], but the conical surface is difficult to fabricate. Alternatively, various tandem systems are used as light-efficient generation of single-mode Bessel fields [10, 11]. However they all need two separated elements, which increases the complexity of the systems. On the other hand, a regular circular grating also generates a conical wave in the first order, which also forms a long focal depth [12–14].

Conventionally generated axicons are reported on a flat substrate, where they tend to generate a conical beam with linearly increasing intensity on axis. If they are fabricated on a curved substrate, their intensity in the beam centre is near constant. Some work on curved diffractive optical elements has been reported [15–17]. We fabricate an amplitude axicon on a concave lens surface using the laser direct writing lithography technique, which has more constant intensity on axis, and far longer focal depth than that fabricated on a flat surface with the same parameter. So we can use this method to get better performances for axicons. In this paper a long focal depth diffractive optical element on a concave lens is demonstrated experimentally.

2. Design

The optical function of the linear axicon is to generate a line focus with increasing axial intensity over some finite range $0 < z < z_1$. By use of the general prescription referred to above, the exact radially symmetric phase function $\phi(r)$ characterizing a circular-aperture forward linear axicon within $0 \leqslant r \leqslant r_1$ is [8]

$$\phi(r) = -k\frac{r}{a^{1/2}} \tag{1}$$

where $a = z_1^2/r_1^2$, $k = 2\pi/\lambda$, where λ is the wavelength of incident light. The optical function of the linear axicon may also be achieved by a circular binary amplitude grating of local period d, which is fabricated on a concave lens

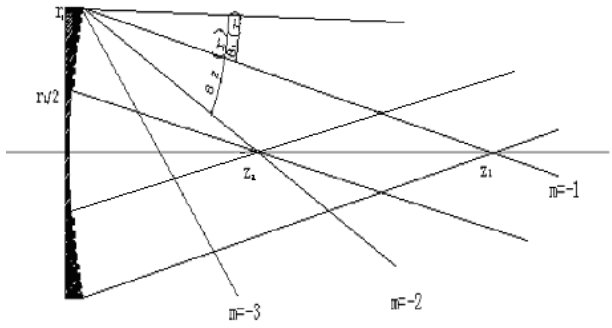

Figure 1. Line focus generated by an annular-aperture diffractive axicon on a plane concave lens.

surface by laser beam lithography as long as the circular binary amplitude grating has the same phase function as the linear axicon. From the grating equation we get $\sin\theta(r) = \lambda/d(r) = -\partial\phi(r)/k\partial r$, where θ is the diffractive angle, so we obtain the period according to equation (1)

$$d(r) = \lambda a^{1/2}. \tag{2}$$

However, because the binary amplitude element is a diffractive element, different orders will interfere with each other within some range. For the first and second diffractive orders, the small diffractive angles can be expressed respectively:

$$\sin\theta_1(r) = -\frac{\partial\phi(r)}{k\partial r} = \frac{1}{a^{1/2}} \approx \tan\theta_1(r) = \frac{r_1}{z_1} \tag{3}$$

$$\sin\theta_2(r) = -2\frac{\partial\phi(r)}{k\partial r} = 2\frac{1}{a^{1/2}} \approx \tan\theta_2(r) = \frac{r_1}{z_2}. \tag{4}$$

So the second order will interfere with the first order within the range $0 < z < z_2$, where $z_2 = r_1 a^{1/2}/2 = z_1/2$ according to equations (3) and (4).

In order to eliminate the interference effects between different diffractive orders (mainly between the first and second orders), we can write the concave substrate within an aperture $r_1/2 \leqslant r \leqslant r_1$, which can generate a line focus with increasing axial intensity over some finite range $z_1/2 < z < z_1$, as illustrated in figure 1. Certainly, some energy is lost in this work, but the loss is much less than that of using a ring aperture for focal line extension.

Now in order to examine the behaviour of the light intensity along the focal range $z_1/2 < z < z_1$, we substitute the phase-retardation function defined by equation (1) into the Fresnel diffraction integral, where the incident wave is a unit light intensity plane wave

$$I(0,z) = \left(\frac{1}{\lambda z}\right)^2 \left| \int_{r_1}^{r_2} \exp\left\{ \mathrm{i}\left[\frac{kr^2}{2z} + \phi(r)\right]\right\} r\,\mathrm{d}r \right|^2. \tag{5}$$

On the other hand, the phase-retardation function needs to be added to another one that is due to the element fabricated on a concave lens surface:

$$\phi'(r) = -kf\left[1 - \left(1 - \frac{r^2}{f^2}\right)^{1/2}\right] \tag{6}$$

where f is the focal length of the lens. For a large $F_\#$ lens, it may be simplified as

$$\phi'(r) = -k\frac{r^2}{2f}. \tag{7}$$

So the new phase-retardation function is given by

$$\phi_1(r) = -k\frac{r^2}{2f} - k\frac{r}{a^{1/2}}. \tag{8}$$

By using the method of stationary-phase analysis, we get the simply axial intensity distribution, the propagation distance range and the full width (diameter of a central lobe of the J_0 Bessel beam) as below. The details of the derivations are shown in the appendix:

$$\frac{r_2}{a^{-1/2} + \frac{r_2}{f}} \leqslant z \leqslant \frac{r_1}{a^{-1/2} + \frac{r_1}{f}} \qquad f < -\frac{r_2}{a^{-1/2}} \tag{9}$$

$$I(z) \approx \frac{k2\pi f^3 z}{a(z-f)^3} \tag{10}$$

$$\rho = \frac{2.4\lambda a^{1/2}}{\pi}\left(1 - \frac{z}{f}\right). \tag{11}$$

According to equations (9)–(11), three conclusions can be drawn. Firstly, the focal length is longer, especially when f nears $-r_1/a^{-1/2}$. Secondly, the intensity on axis varies with z along a nonlinearity function. This is not constant, but it happens that the propagation range z_1 to z_2 is around the maximum of the function when f chosen correctly, and thus it varies only a little in this range. Lastly, the full width increases with z. The bigger f is chosen, the more obvious the increment is. So when using this kind of diffractive axicon, f should be balanced.

The computer simulation result for a plane concave lens with the parameters $\lambda = 632.8$ nm, $r_1 = 20$ mm, $r_2 = 10$ mm, $z_1 = 316.06$ mm, $z_2 = 158.03$ mm, $R_1 = 0$ mm (radius of the front surface of the plane concave lens), $R_2 = 462.484$ mm (radius of the rear surface of the lens) and $n = 1.5168$ (refractive index of the lens) for $f = -839.04$ mm (focal length of the length) is presented in figure 2(a), and the result with the same parameters except for $R_2 = 0$ and $f = \propto$ mm is presented in figure 2(b).

Figure 2 shows the intensity distribution along the z axis in the focal range of the diffractive optical element fabricated on a concave lens surface. For comparison, we also present the corresponding distribution of one on a flat surface. As is evident, the focal depth for the diffractive axicon on the concave surface is two times greater than that on a flat surface. As expected, the peak intensity is lower by approximately the same factor of the focal length changes and its energy distribution along axis is more uniform. However, the average intensity oscillates severely in the beginning of the focal line, which may be caused by the interference effects between the second-order and the first-order diffracted light.

3. Fabrication and experiment

We have fabricated a long focal length diffractive axicon pattern onto a concave lens surface with precise alignment by

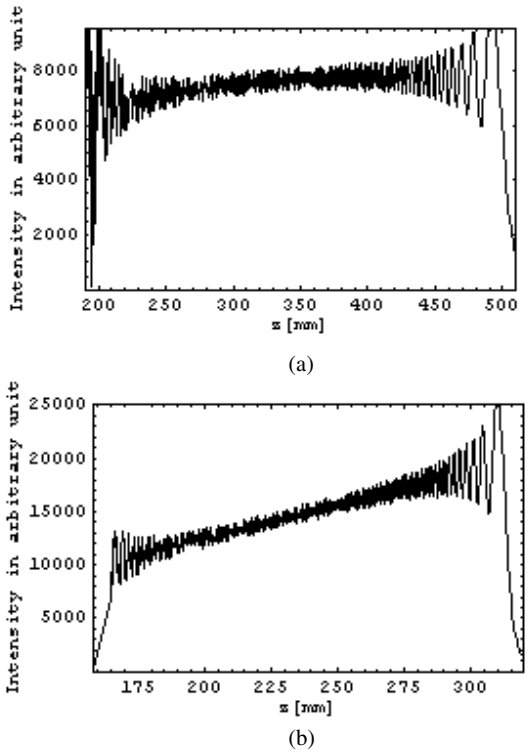

Figure 2. On-axis intensity distribution for diffractive axicon with $\lambda = 632.8$ nm, $r_1 = 20$ mm, $r_2 = 10$ mm, $z_1 = 316.06$ mm, $z_2 = 158.03$ mm, $R_1 = 0$ mm, $R_2 = 462.484$ mm, $n = 1.5168$ and $f = -839.04$ mm. (a) On-axis intensity distribution for diffractive axicon with $\lambda = 632.8$ nm, $r_1 = 20$ mm, $r_2 = 10$ mm, $z_1 = 316.06$ mm, $z_2 = 158.03$ mm, $R_1 = 0$ mm, $R_2 = 0$ mm, $n = 1.5168$ and $f = \propto$ mm (b).

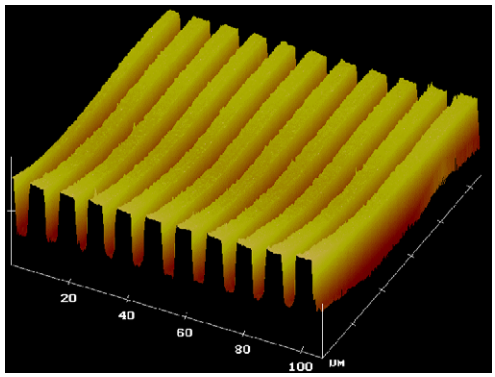

Figure 3. Three-dimensional plot of the grating profile obtained by atomic force microscope.
(This figure is in colour only in the electronic version)

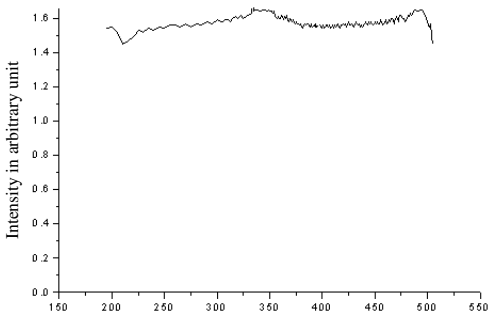

Figure 4. Measured axial intensity distribution of a diffractive axicon with $\lambda = 632.8$ nm, $r_1 = 20$ mm, $r_2 = 10$ mm, $z_1 = 316.06$ mm, $z_2 = 158.03$ mm, and $R_1 = 0$, $R_2 = 462.484$ and $n = 1.5168$ for $f = -839.04$ mm.

using our laser direct writer [18]. We used a 150 mW He–Cd laser at a wavelength of 442 nm. Stage movement was controlled to a precision of 0.2 μm in three Cartesian axes by use of feedback from distance measurement with linear encoders from Heidenhain GmbH. The concave substrate coated by S1813 Microposit photoresist film of about 0.9 μm height is aligned with the air-bearing spindle by means of a high-precision alignment apparatus. We aligned the axis of the optical head assembly with the air-bearing spindle's centre of rotation based on a rotating linear grating [19].

Then the circular patterns are optimally fabricated using polar coordinate machines that expose rings by rotating the substrate under a fixed writing beam. After writing, the optic is immersed into a solution of NaOH to dissolve the exposed photoresist, and the pattern of bare photoresist remains. By using an atomic force microscope, a three-dimensional plot of the line profiles of the grating with a 10 μm period is shown in figure 3. Because the pattern of photoresist is difficult to retain longer, we form a pattern in chrome by using the method of pattern transfer. Chrome is plated on the surface of the optic, and then the optic is immersed into solution to dissolve the remained photoresist. So after development, a diffractive axicon pattern of chrome is formed. In our experiment, the concave substrate is 40 mm in diameter, which has a radius of curvature of 462.484 mm and refractive index of 1.5168. So the focal length of the concave lens is -839.04 mm when $\lambda = 632.8$ nm. We write the diffractive axicon pattern on the concave lens surface from 10 to 20 mm in radii. The writer accuracy can be controlled to 0.5 μm, so the precision of 1/20 can be realized per 2π phase shift for the diffractive grating.

In the experiment, the axicon was illuminated with a uniform plane wave derived from a He–Ne laser of $\lambda = 633$ nm. An optical power detector with 1 mm in diameter was used to monitor the transverse average intensity distribution. The meter was moved step by step over a range that exceeded the theoretical extent of the line focus. In each step the transverse average intensity was recorded. The average intensity distribution along the axis is presented in figure 4. By comparison of these experimental results with the numerical results of figure 2(a), it is evident that good agreement exists. The ripples in figure 4 are caused by the oscillations of on-axis intensity of the generated long focal beam.

4. Discussion and conclusion

We have shown that a linear axicon can be designed as a binary-amplitude element and fabricated on a concave lens surface with precise alignment by using a laser direct writer. The effectiveness of the new element was demonstrated. Not only is focal depth much longer than that fabricated on a flat surface with the same parameter, but also energy distribution along axis is more uniform. Moreover, the approach is also valid for

small $F_{\#}$, but the paraxial approximation of equation (7) may no longer be valid, and equation (6) must be used directly.

There remains some room for improvements, however. For example, the results show prominent rapid oscillations of the on-axis intensity within the focal region. The oscillations are naturally interpreted as a result of interference of the main conical wave with a boundary diffraction wave generated at the sharp edge of the aperture. Therefore the oscillation strength could be significantly reduced if an apodized illumination [13, 20] is employed. Secondly, only some 10% of the light incident upon the annular aperture of the diffractive axicon can be utilized. Multi-level diffractive axicon can improve light efficiency to 40% [21], but it is more complex to fabricate it. In order to get more uniform intensity distribution along the axis, an axicon illuminated with a Gaussian beam can be used [22].

Acknowledgments

This study is supported by the National Natural Science Foundation (60577004) and State Key Laboratory of Applied Optics.

Appendix

The field distribution behind the diffractive axicon on a curved surface can be determined through the Fresnel diffraction integral:

$$u(\rho, z) = \frac{2\pi}{\lambda z}\int_{r_2}^{r_1} \exp\left[ki\left(\frac{r^2}{2z}+\frac{r^2}{2f}-a^{-1/2}r\right)\right] \times J_0\left(\frac{2\pi\rho r}{\lambda z}\right) r\,\mathrm{d}r \tag{A.1}$$

where the common phase factor $\exp(ikz)$ is omitted. So the axial field of this beam (at $\rho = 0$) takes the form

$$u(0, z) = \frac{2\pi}{\lambda z}\int_{r_2}^{r_1} \exp\left[ki\left(\frac{r^2}{2z}+\frac{r^2}{2f}-a^{-1/2}r\right)\right] r\,\mathrm{d}r. \tag{A.2}$$

According to the stationary phase method [23, 24], when the first terms of an asymptotic expansion are used, the following representation is valid [25]:

$$\int_a^b f(t)\exp[\mathrm{i}K\mu(t)]\,\mathrm{d}t \approx f(t_s)\left[\frac{2\pi}{K\mu''(t_s)}\right]^2 \exp\left\{\mathrm{i}\left[K\mu(t_s)+\frac{\pi}{4}\right]\right\} + \frac{f(t)}{\mathrm{i}K\mu'(t)}\exp\left[\mathrm{i}K\mu(t)\right]|_a^b, \qquad t_s \in (a, b). \tag{A.3}$$

Provided that $K \to \infty$, $\mu''(t_s) > 0$, $\mu'(a) \neq 0$ and $\mu'(b) \neq 0$, where $f(t)$ and $\mu(t)$ are monotonic functions slowly varying within an integration region against the argument t, $\mu'(t)$ and $\mu''(t)$ denote the first and second derivatives of $\mu(t)$, while t_s is a single-valued stationary-phase point derived from the equation

$$\mu'(t_s) = 0. \tag{A.4}$$

Applying asymptotic representation (A.3) to integral (A.2), we derive an expression involving two terms only as

$$U(0, z) = U_g(z)\exp[\mathrm{i}\phi_g(z)] + U_b(z)\exp[\mathrm{i}\phi_b(z)] \tag{A.5a}$$

where

$$U_g(z) = \frac{kr_s}{z}\left[\frac{2\pi f z}{k(z+f)}\right]^{1/2} \tag{A.5b}$$

$$U_b(z) = -\frac{r_1}{z(\frac{z+f}{zf}r_1 - a^{-1/2})} + \frac{r_2}{z(\frac{z+f}{zf}r_2 - a^{-1/2})} \tag{A.5c}$$

$$\phi_g(z) = \frac{kr_s^2}{2z} + \frac{kr_s^2}{2f} - ka^{-1/2}r_s - \frac{\pi}{4} \tag{A.5d}$$

$$\phi_b(z) = \frac{kr_1^2}{2z} + \frac{kr_1^2}{2f} - ka^{-1/2}r_1 + \frac{\pi}{2} - \frac{kr_2^2}{2z} - \frac{kr_2^2}{2f} + ka^{-1/2}r_2. \tag{A.5e}$$

$U_g(z)$, $U_b(z)$ and $U_{bg}(z)$ stand for the amplitude components of the geometrical, boundary and interference components of the axial intensity, respectively. In which the geometrical component contribution to the axial intensity is the main part. From equation (A.4) we can derive radial stationary-phase points r_s

$$r_s = \frac{a^{-1/2}zf}{z+f}. \tag{A.6}$$

So the axial intensity distribution may be simplified as

$$I(0, z) \approx \frac{k2\pi f^3 z}{a(z-f)^3}. \tag{A.7}$$

According to equation (A.6), the propagation distance range is found to be

$$\frac{r_2}{a^{-1/2}+\frac{r_2}{f}} \leqslant z \leqslant \frac{r_1}{a^{-1/2}+\frac{r_1}{f}} \qquad f < -\frac{r_2}{a^{-1/2}}. \tag{A.8}$$

The full width (diameter of a central lobe) is determined by the characteristic of the J_0 Bessel beam:

$$\frac{2\pi\rho\, r_s}{\lambda z} = 2.4. \tag{A.9}$$

Substitution of equation (A.6) into (A.9) yields

$$\rho = \frac{2.4\lambda}{2\pi\beta_0}\left(1+\frac{z}{R}\right). \tag{A.10}$$

References

[1] Mcleod J H 1960 Axicons and their uses *J. Opt. Soc. Am.* **50** 166–9
[2] Mcleod J H 1954 Axicon: a new type of optical element *J. Opt. Soc. Am.* **44** 592–7
[3] Tremblay R, D'Astous Y, Boand G and Blanchard M 1979 Laser plasmas optically pumped by focusing with an axicon a CO_2-TEA laser beam in a high-pressure gas *Opt. Commun.* **28** 193–6
[4] Hausler G and Heckel W 1988 Light sectioning with large depth and high resolution *Appl. Opt.* **27** 5165–9
[5] Rioux M, Tremblay R and Belanger P 1978 Linear annular and radial focusing with axicons and applications to laser machining *Appl. Opt.* **17** 1532–6
[6] Indebetouw G 1989 Nondiffracting optical fields: some remarks on their analysis and synthesis *J. Opt. Soc. Am.* A **6** 150–2
[7] Fujiwara S J 1962 Optical properties of conic surfaces. I. Reflecting cone *Opt. Soc. Am.* **52** 287–92
[8] Herman R and Wiggins T 1991 Production and uses of diffractionless beams *J. Opt. Soc. Am.* A **8** 932–42

[9] lt J and Dholakia K 2000 Generation of higher-order Bessel beams by use of an axicon *Opt. Commun.* **177** 297–301
[10] Sedukhin A G 1998 Beam-preshaping axicon focusing *J. Opt. Soc. Am.* A **15** 3057
[11] Honkanen M and Turunen J 1998 Tandem systems for efficient generation of uniform-axial intensity Bessel fields *Opt. Commun.* **154** 368–75
[12] Friberg A T 1996 Stationary-phase analysis of generalized axicons *J. Opt. Soc. Am.* A **13** 743–50
[13] Perez M V, Gomez-Reino C and Caudrado J M 1986 Diffraction patterns and zone plates produced by thin linear axicons *Opt. Acta* **33** 1161–76
[14] Vasara A, Turunen J and Friberg A T 1989 Realisation of general non-diffracting beams with computer-generated holograms *J. Opt. Soc.* **46** 1748–54
[15] Bokor N and Davidson N 2005 Curved diffractive optical elements *Design Appl. Prog. Opt.* **48** 107–48
[16] Bokor N and Davidson N 2001 Aberration-free imaging with an aplanatic curved diffractive element *Appl. Opt.* **40** 5825–9
[17] Liu H, Lu Z, Li F, Xie Y, Kan S and Wang S 2004 Using curved hologram to test large-aperture convex surface *Opt. Express* **12** 3251–5
[18] Xie Y, Lu Z, Li F, Zhao J and Weng Z 2002 Lithographic fabrication of large diffractive optical elements on a concave lens surface *Opt. Express* **10** 1043–7
[19] Milster T D and Vernold C L 1995 Technique for aligning optical and mechanical axes based on a rotating linear grating *Opt. Eng.* **34** 2840–4
[20] Vasara A, Turunen J and Friberg A T 1989 Realization of general nondiffracting berms with computer-generated holograms *J. Opt. Soc. Am.* A **6** 1748–54
[21] Popov S Yu, Friberg A T, Honkanen M, Lautanen J, Turunen J and Schnabel B 1998 Apodized annular-aperture diffractive axicons fabricated by continuous-pathcontrol electron beam lithography *Opt. Commun.* **154** 359–67
[22] Xiong P J, Huihua Z and Shojiro N 2000 Lens axicons illuminated by Gaussian beams for generation of uniform-axial intensity Bessel fields *Opt. Eng.* **39** 803–7
[23] Papoulis A 1968 *Systems and Transforms with Application in Optics* 1st edn (New York: McGraw-Hill) chapter 7
[24] Stammes J J 1986 *Waves in Focal Regions* (Bristol: Hilger) chapters 8 and 9
[25] Sedukhin A G 2000 Marginal phase correction of truncated Bessel beams *J. Opt. Soc. Am.* A **17** 1059–66